Fusion Engineering and Design 219 (2025) 115234

Contents lists available at ScienceDirect

Fusion Engineering and Design

journal homepage: www.elsevier.com/locate/fusengdes

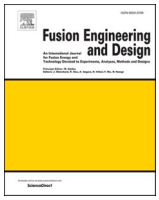

Hydraulic analysis of the DTT divertor module

Davide Caprini [a,1,*], Morena Angelucci [a,1], Emanuela Martelli [a,1], Fabio Crescenzi [a], Francesco Giorgetti [a,b], Nicola Massanova [c], Pietro Vinoni [c], Domenico Marzullo [c], Selanna Roccella [a]

[a] ENEA, Nuclear department, NUC-FUSEN-TES, Frascati, Italy
[b] DTT s.c.a.r.l., Frascati, Italy
[c] CREATE Consortium, Department of engineering and architecture, University of Trieste, Trieste, Italy

ARTICLE INFO

Keywords:
DTT
Cassette
Divertor
Critical heat flux
Hydraulic analysis

ABSTRACT

Understanding coolant flow behaviour in the divertor module is critical for managing the high thermal loads encountered in Tokamak plasma scenarios. Effective cooling ensures system integrity, optimal performance, and prolonged component lifetime, especially in high-heat flux environments. This study investigates the hydraulic performance of the DTT (Divertor Tokamak Test) divertor module, focusing on achieving uniform flow distribution.

The DTT facility, under construction at ENEA C.R. Frascati, is designed to explore power exhaust solutions for DEMO. The initial DTT divertor comprises 54 water-cooled modules, each handling a total mass flow rate of 577 kg/s with water temperatures ranging here considered from 30 °C to 74 °C. Each module includes an Outer Target (OT), Inner Target (IT), and Central Target (CT), with coolant entering through an outboard manifold and flowing through nine OT tubes. Two of the external pipes return directly to the outlet manifold, while the remaining pipes continue through additional components, necessitating calibrated orifices to achieve balanced flow distribution.

A Computational Fluid Dynamics (CFD) model was developed to optimize orifice sizing in OT pipes and evaluate flow uniformity. Sensitivity analyses assessed the effects of bulk water temperature variations and manufacturing tolerances on orifice dimensions. The model also examined total pressure drops and localized losses caused by twisted tapes in the tubes promoting flow swirling. Finally, the impact of flow rate fluctuations on critical heat flux was analysed, offering insights into the hydraulic system robustness under variable conditions. Simulations were performed using ANSYS software, providing an evaluation of the divertor module cooling performance.

1. Introduction

In a Tokamak, the divertor plays a vital role in managing the intense heat generated during plasma confinement. The divertor is responsible for absorbing the thermal load produced in various plasma conditions, ensuring the safe operation of the reactor. This makes the divertor cooling system a key element in maintaining the structural integrity of the device, especially in high-heat flux environments. Effective cooling is not only essential for keeping the reactor within operational temperature limits, but also for enhancing the longevity and reliability of its components. A malfunction or inefficiency in the divertor cooling system could lead to overheating, material degradation, or even failure of critical parts. Therefore, the design and optimization of the cooling process is of paramount importance.

The divertor cooling system must address the unique challenges posed by the complex geometry of the divertor module and the extreme heat conditions it faces. The divertor module, composed of plasma-facing surfaces connected by tubes and a cassette, requires a precise and controlled flow of coolant to absorb the heat generated during operation. The coolant, usually water, flows through the system via a network of tubes designed to maintain an even distribution of temperature across the entire module. If the coolant does not flow evenly, certain areas could experience higher thermal gradients, leading to localized overheating and potentially compromising the performance of

* Corresponding author.
E-mail address: davide.caprini@enea.it (D. Caprini).
[1] These authors have contributed equally.

https://doi.org/10.1016/j.fusengdes.2025.115234
Received 16 January 2025; Received in revised form 8 May 2025; Accepted 27 May 2025
Available online 14 June 2025

the divertor as a whole.

In the specific case of the Divertor Tokamak Test (DTT) facility [1,2], which is currently being constructed at ENEA C.R. Frascati, the divertor cooling system is designed to explore alternative power exhaust strategies for future Tokamak designs, particularly those relevant to the DEMO project [2–5]. The first DTT divertor will be composed of 54 modules, each cooled by water with an inlet temperature ranging from 30 °C to 60 °C plus a contribution due to heating. Indeed, when the divertor reaches the designed thermal load at the critical heat flux limit, the water temperature rises to approximately 74 °C. The water is fed in parallel to the modules, with 50 Bar of pressure and a total mass flow rate of 577 kg/s [6].

The water flow rate required to supply each module, in order to effectively remove heat at an average temperature of 60 °C, must be 10.68 kg/s. This flow ensures that the heat is efficiently transferred away from the system, maintaining the necessary thermal balance for optimal operation.

In the context of high-flow testing, a mass flow rate of 10.68 kg/s for each tube was established, driven by the necessity to achieve a velocity of approximately 11 m/s within 12 mm diameter tubes. This velocity is important to ensure a safety margin against reaching critical heat flux conditions under the stationary operating load of 20 Mw/m^2 on the divertor targets. The selected flow rate not only optimizes system performance but also mitigates the risks associated with flow instabilities that could arise at lower velocities.

The high mass flow rate, coupled with the varying temperature of the coolant, poses significant design challenges in terms of ensuring that the heat is efficiently removed from each module without creating imbalances in the cooling system. A critical aspect of this design involves ensuring that the coolant is evenly distributed across the different sections of the divertor. Inconsistent flow rates or localized blockages could lead to areas of the divertor being exposed to higher temperatures than intended. To address this, the DTT design includes measures such as calibrated orifices in the external pipes of the Outer Target, Fig. 1, which help regulate the flow and ensure that each cooling channel receives an appropriate share of the coolant.

The hydraulic performance of the divertor cooling system is, therefore, a primary focus of this study. Computational Fluid Dynamics (CFD) modelling is employed to simulate the flow of coolant through the module and to analyse factors such as pressure drops, flow distribution, and temperature variations [7,8]. The goal is to fine-tune the system so that it achieves a balanced flow across all sections of the divertor, even under the most demanding operational conditions. By addressing these design challenges, the DTT facility aims to provide valuable insights for the future development of high-performance cooling systems in fusion reactors.

2. Description and characteristics of the fluid domain

In the cooling system, water is circulated through each module by a pumping system, which directs it first into an inlet manifold and then distributes it to the pipes of the plasma facing units. The water flows sequentially through the three plasma-facing units, where it absorbs heat before being collected by the outlet manifold. From there, the water is channelled back through the box-like structure of the cassette and directed toward the outlet manifold (see Fig. 1).

To enhance heat transfer between the cooling fluid and the inner walls of the pipes, copper swirl tapes are inserted inside the straight sections of the tubes namely the target. The swirls are made of copper and are pre-inserted into the tubes, for a length of 200 mm with a thickness of 0.8 mm and swirl ratio (pitch/2*diameter) equal 2. These swirls induce a swirling motion in the water, which increases heat transfer by promoting turbulence in the flow. In addition, the copper spirals are in direct contact with the inner surface of the tube, ensuring maximum heat transfer.

Fig. 2 shows a cross-section of the complete divertor module. The lengths of the targets are reported. The swirls are positioned in the straight sections of the outer target and the inner target, which are those designed for the highest thermal load.

This configuration allows for optimized thermal management, crucial in maintaining the structural integrity of the plasma-facing components, as it prevents overheating and ensures the system's ability to withstand high thermal loads during operation. The combination of sequential water flow through the units and the turbulence-enhancing

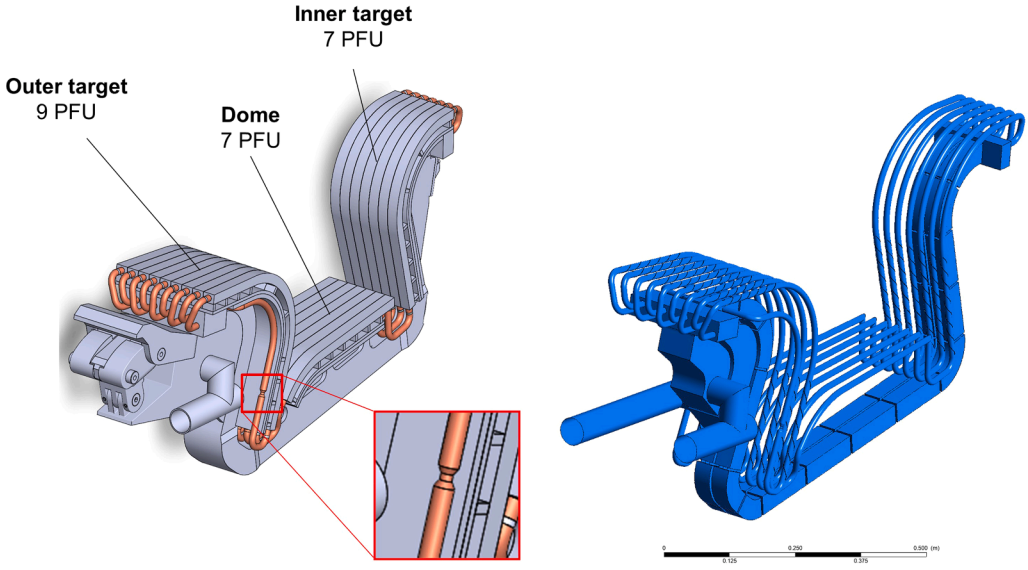

Fig. 1. On the left, the 3D cassette model of the DTT divertor is shown, highlighting the three main targets: outer target (OT), dome or central target (CT), and inner target (IT). The zoomed-in detail illustrates how, to transition from the 9 tubes of the OT to the 7 tubes of the CT and IT, constrictions are applied to the two outer tubes to balance the flow across all targets. On the right, the volume of pressurized water filling the divertor cassette module, which is the fluid domain of this study, is displayed. Total scale bar length is 0,5 m.

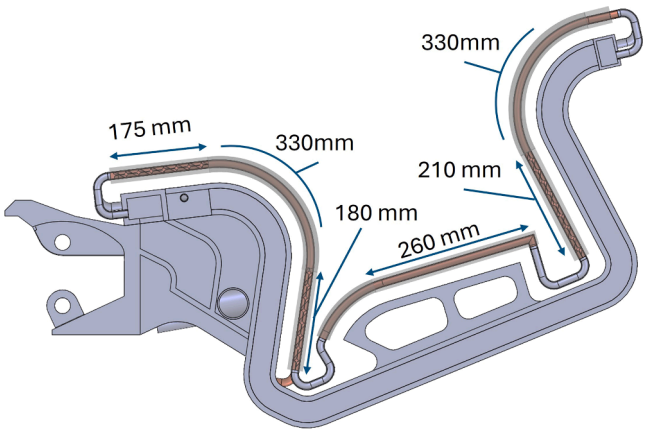

Fig. 2. Mid-section of the divertor module with the main length of the targets facing the plasma. The section view of the central tube shows the presence of swirls in the vertical and horizontal straight part of the outer target and in the vertical part of the inner target, which are designed for the highest thermal stress.

copper spirals inside the pipes contributes significantly to the overall cooling efficiency, ensuring effective temperature regulation and the longevity of the plasma-facing surfaces.

3. Mesh and CFD model

A preliminary sensitivity study on grid was conducted using a simplified model, without any refinement applied at the walls. This approach allowed for a general evaluation of the influence of mesh density on the results while optimizing computational resources. The maximum element size varied from 4 mm to 1 mm. Across these variations, the observed difference in calculated pressure drops among the cases were minimal, with a maximum variation of 3 %, see Fig. 3d).

The grid parameters for the complete model were selected as a compromise between the sensitivity analysis results and computational costs. For the final CFD model, the maximum cell size was set at 1 mm for the pipes and 2 mm for the cassette ducts and manifolds. The grid is conformal in all the interfaces and mainly composed by tetrahedral elements. Hexahedral cells are used to refine the discretization at the walls for a more detailed assessment of the boundary layer. Reynolds-Averaged Navier-Stokes (RANS) turbulent model with SST k-ω turbulence closure model is used and particular attention was paid to the control of the $Y+$ parameter in the various areas of the walls [9]. In order to keep the $y+$ around 1, in accordance with SST turbulence model, the first layer thickness of the mesh was established at 5 μm for the walls of the pipes, for the walls of the cassette and manifolds. Other local refinements were also used somewhere. The total number of elements is about 71 M, whereas the number of nodes is about 27 M.

The boundary conditions set for the solution are a constant flow rate on the inlet manifold section and no-slip wall. On the outlet section, the pressure is constant and equal to the reference one. The wall roughness is 3.0e-6 m.

The advection scheme is an upwind roughness, and the RMS residual convergence criterion was set to a target value of 1.0e-7 and the actual residuals were about 1.0e-5. This configuration was chosen to provide sufficient detail in regions of high gradient while keeping the total cell count manageable and guarantee the convergence of the simulation. Overall, this grid setup enables accurate prediction of flow behaviour within the divertor module while maintaining computational efficiency.

The simulations were made by running the model at three different temperatures of 30 °C, 60 °C and 74 °C, at 50 bar of pressure. The different effect on the characteristics of the water was made by changing the values of density and viscosity in the characteristics of the fluid. The data were taken using an open source water thermodynamic characteristics variability model through the Calc-steam software. For each hydraulic simulation, a constant flow rate of 10.68 kg/s was imposed as boundary condition at the inlet section of the main manifold, in accordance with the specifications required for the module cooling system, and a constant pressure condition, equal to the reference pressure, was used at the outlet section.

4. Results

The CFD simulations conducted in ANSYS 2022 R1 using the Fluid

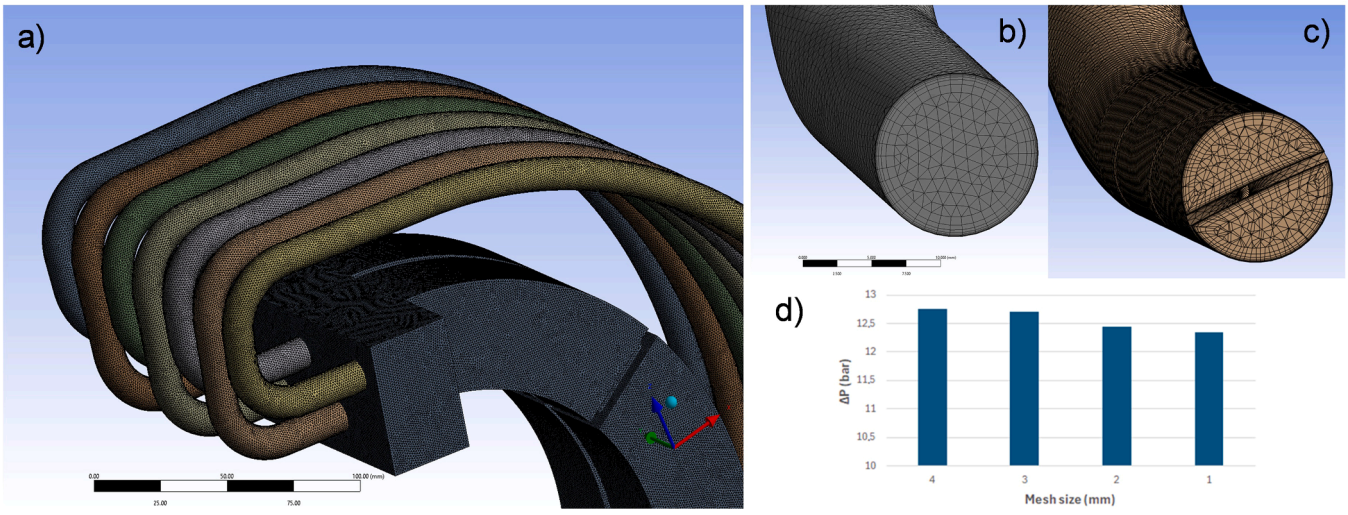

Fig. 3. a) The mesh of the CFD simulation for the divertor cassette is shown, focusing on the tubes exiting the feeding manifold. The mesh follows refinement rules in critical areas of the domain. b) Cross-section of the tube without swirl. c) Cross-section of the tube with swirl. Figures highlight the inflation of the wall-adjacent mesh for accurate boundary layer calculations. Particular attention was paid to the control of the $Y+$ parameter in the various areas of the walls. Care was taken to always keep it around 1 in accordance with the SST turbulence model closure. d) Trend of the pressure drop obtained in the cassette module is shown as a function of the maximum size of the mesh elements. The pressure variation changes little, especially between 4 and 3 mm , favoring a reduction in computational effort.

Flow (CFX) software provided insights into the flow distribution and pressure drops within the divertor module under varying operating conditions. Initial results indicated that the orifice calibration in the OT external tubes was essential in maintaining an even flow distribution. The calibrated orifice size helped minimize flow imbalance among the cooling channels, even in sections where turbulence was introduced through copper swirls. The sensitivity analysis revealed that the bulk temperature of the coolant significantly affects the orifice size, as higher temperatures tend to decrease the fluid viscosity, potentially resulting in increased flow rates. Moreover, manufacturing tolerances in the pipe dimensions were found to have a notable impact on the orifice design, underscoring the importance of precise manufacturing controls in achieving optimal hydraulic performance.

The Fig. 4 demonstrates that an effective flow rate balance among the outer tubes is achieved using an orifice with a radius of 2.7 mm. This configuration ensures flow rate variations between the tubes are limited to only a few percentage points (max 4 %). The percentage is the value of the deviation normalized with the mean average. Additionally, it highlights that the flow balance remains unaffected by changes in temperature, and thus, it is independent of variations in fluid density and viscosity. From the trend it is clear that decreasing the orifice diameter an excessive restriction of the flow is generated in the side tubes and therefore there is an inversion of the effect on the global balance. Thus, it is correct to have the minimum radius around 2.7 mm., Fig. 4b).

From the flow lines shown in Fig. 5, we can observe the formation of stagnation points inside the distribution manifold. These points are bypassed by the flow, causing a slight imbalance in the flow rates of the pipes. These zones cause flow imbalances, even in the inner tubes, which lack constrictions. However, analysis of the results indicates that these recirculation zones induce only minor flow rate variations, remaining below 4 % as mentioned above.

If we define the ideal design velocity as the velocity obtained by dividing the flow rate of a single module by 9 (1186 Kg/s) in the outer target, we find value of 11,7 m/s mean value. This velocity corresponds to the calculated velocity based on the cross-sectional area of the tube in the targets where swirl is present (without swirl 10,73 m/s mean value).

The study also evaluated the total pressure drop across the module component and the velocity magnitude images confirm that in the tube, the magnitude varies from 11 m/s to approximately 18 m/s along the 90-degree curve (see Fig. 6).

Meanwhile, the pressure variation along the tube is more pronounced in the regions where the swirls are present. From the pressure and velocity trends in the tube Fig. 6a and b we verify that we are in line with the estimated average values. The images show a central tube without restriction. In Fig. 6b and d instead, we can see that in the cassette module the pressure drop occurs in a discontinuous manner due to the lateral partitions. Regarding the velocity, the streamlines show a trend approximately constant with few recirculation zones downstream of the bulkheads.

Based on such hydraulic results, we moved to the evaluation of the critical heat flux and the relative safety margin under the design thermal loads and considering the monoblock geometry. The pipe Critical Heat Flux (CHF) was calculated, by Tong-CEA correlations based on pipe geometry and fluid properties. Before FEM thermal analysis, critical monoblock geometries were selected for different targets, i.e. the one with the largest toroidal width. Ansys mechanical simulations applied the Incident Heat Flux on plasma facing surface of the monoblock and a temperature-dependent Heat Transfer Coefficient (HTC) at the pipe surface to determine flux concentration.

The HTC is a function of the temperature at the tube wall and was obtained through the CEA Thermoprop software developed in the 90 s (initially its name was EUPITER) [10–13]. In this code, to determine HTC as a function of temperature, 4 correlations are used and interpolated among them, allowing to obtain a good estimate of the temperature and heat flux from the FEM solution for any heat exchange regime and also in conditions close to CHF(see Rabaglino [13]).

In Table 1, the velocity values and the design load are reported. The design load is 20 MW/mˆ2 for the inner and outer vertical targets as for outer horizontal targets where the twisted tape is present, while it is 16 MW/m^2 for the central horizontal target (CHT) without twisted tape [14, 15].

In the last column the margin from the CHF wich is the ratio between the ICHF and the design load, is reported. It is the typical value used in this type of components [15].

5. Conclusion

This study demonstrates the feasibility of achieving a balanced coolant flow in the divertor cooling system of the DTT facility through careful calibration of orifice sizes and the use of CFD modelling. The sensitivity analysis confirmed that both bulk water temperature and orifice dimensions could be accommodated without compromising the system performance. The investigation provided detailed insights into the flow distribution, pressure drops, and thermal behaviour of the divertor module cooling system under variable operational conditions. The analysis confirmed that calibrated orifices are essential for achieving a balanced coolant flow across the Outer Target (OT) tubes, ensuring thermal uniformity and avoiding localized overheating.

a)

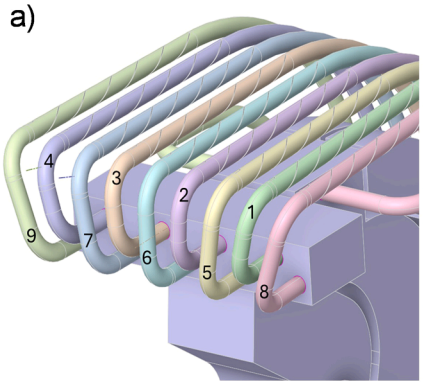

Tube number	Flow rate kg/s at T=30° C	Flow rate kg/s at T=60° C	Flow rate kg/s at T=74° C
1	1.1960	1.194	1.200
2	1.1750	1.176	1.199
3	1.1790	1.177	1.203
4	1.2140	1.217	1.238
5	1.1890	1.192	1.210
6	1,1870	1.187	1.211
7	1.1810	1.182	1.140
8	1.1700	1.167	1.190
9	1.1800	1.180	1.189
Max variation	2.39%	2.63%	4%

b)

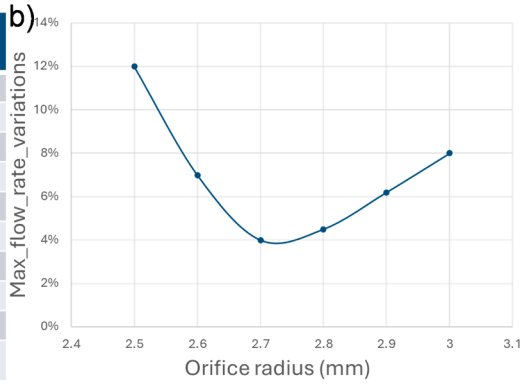

Fig. 4. a) the numbering of the tubes from the manifold to the outer target is shown, and the table reports the flow rate values in the 9 tubes following the correct sizing of the orifice ($r = 2.7$ mm) for the two lateral tubes, 8 and 9. It can be observed that, at the three different temperatures that were tested in the simulation 30 °C, 60 °C and 74 °C, the variation is limited to a few percentage points, indicating that the system can be considered in equilibrium. b) Trend of maximum percentage fluctuations between outer target tubes as a function of orifice radius at 74 °C temperature condition.

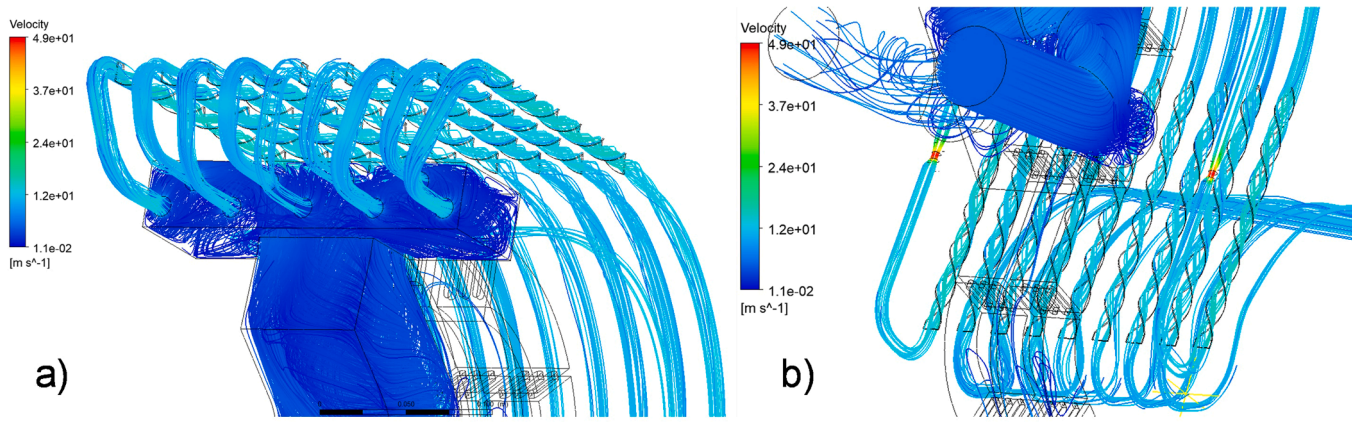

Fig. 5. Images of streamlines and velocity magnitude at 60 °C of temperature. a) Behavior of streamlines in the distribution manifold to the pipes. Small differences in the flow rate of the pipes could be introduced by circulatory behavior in certain flow regions. b) Detail of the behavior of streamlines within the pipes, where the velocity magnitude is confirmed to vary from 11 m/s to higher values due to swirl effects. It can be observed that the velocity is very high in the restriction, which causes the greater pressure loss typical of the two lateral pipes of the external target.

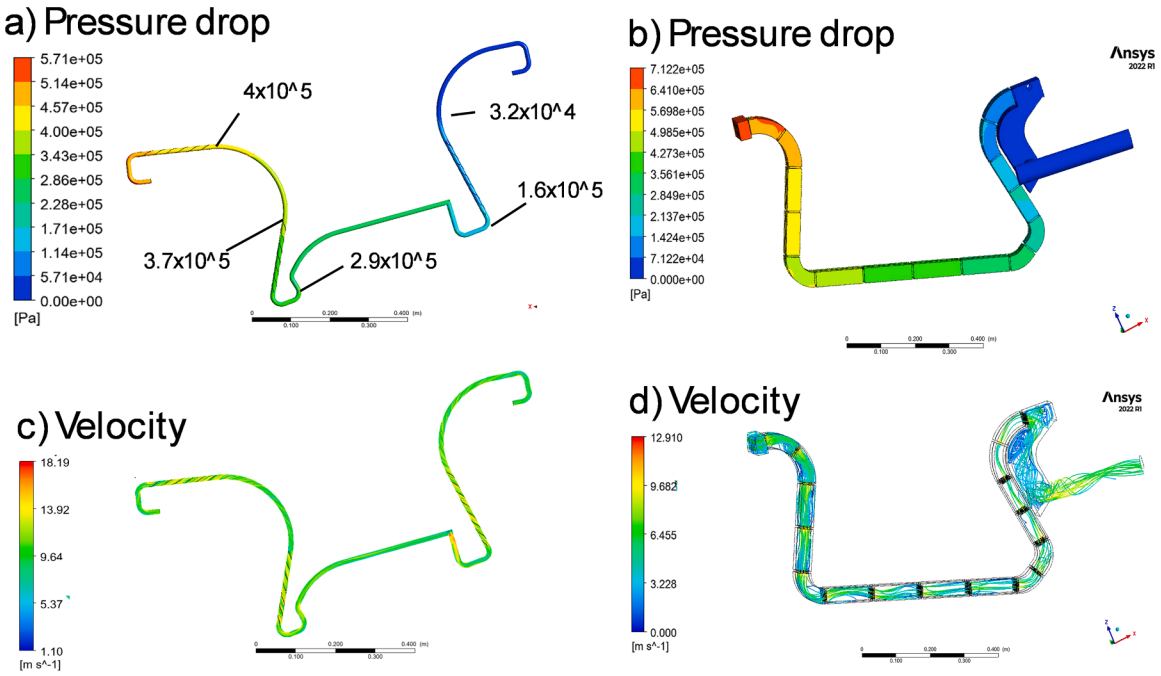

Fig. 6. Pressure drop and Velocity Trends in the Pipe and Cassette Body at 60 °C of temperature. a) Pressure drop Trend in a Central Pipe (number 6) and some numerical values along centre line of the tube. The pressure variation along one of the central pipes is observed. Rapid variations occur in the presence of swirls, which induce a greater pressure drop compared to an empty pipe. The pressure drop in the single pipe is approximately 5 Bar b) Pressure Trend in the Cassette Body. The presence of baffles causes discontinuous pressure variations, as the baffles induce localized pressure losses. c) Velocity Trend in a Central Pipe. The velocity is confirmed to be approximately 11 m/s in the swirl targets, with an increase due to the 90-degree elbow. d) Velocity Visualization Through Streamlines in cassette body.

Key findings revealed that flow imbalances, introduced by recirculation zones in the distribution manifold, remained within acceptable limits (about 4 %), while the copper swirl inserts significantly enhanced thermal exchange by inducing turbulence, a critical requirement for handling the intense thermal load generated in a Tokamak environment.

The study also validated the cooling system ability to maintain a safety margin of 1.4 under design thermal loads, confirming its robustness against critical heat flux conditions. Pressure and velocity trends indicated that the system effectively manages the thermal and hydraulic stresses imposed by the reactor's high-power demands. These findings contribute valuable design strategies for future fusion reactors, enhancing their reliability and longevity under extreme conditions.

The insights obtained from this analysis will contribute to optimizing the divertor cooling systems for future high-performance fusion reactors, supporting the development of robust power exhaust solutions for DEMO and subsequent fusion energy systems.

Table 1
In the table, the critical parameter values at 74 °C and 50 Bar for the divertor module targets are reported. Specifically, the horizontal (OHT) and vertical (OVT) targets of the external target, and the vertical one of the internal target, all equipped with a swirl and designed for a thermal load of 20 MW/m^2. For the central target, however, the design thermal load is 16 MW/m^2. For each target, the following values are reported in order: the average velocity perpendicular to the tube surface, the critical incident load on the tungsten surface, the critical monoblock width, the heat flux concentration factor, the heat flux on the wall pipe due to the corresponding design load, and the value of the critical heat flux induced by the monoblock geometry and thus by a specific concentration factor. Finally, in the last column, the safety margin from the critical heat flux under the design load is shown.

	Design Load (MW/m^2)	Perpendicular velocity (m/s)	ICHF on Tungsten (Mw/m^2)	Critical Monoblock width (mm)	Heat Flux concentration factor	HF at Wall pipe (MW/m^2)	CHF at Wall pipe (MW/m^2)	Margin to Critical Heat Flux
OHT	20	11.73	32.09	29	1.83	36.6	58.7	1.6
OVT	20	11.73	33.42	25.3	1.76	35.2	58.7	1.7
CHT	16	10.73	21.85	30	1.83	29.3	40	1.4
IVT	20	11.73	33.77	25.8	1.74	34.8	58.7	1.7

CRediT authorship contribution statement

Davide Caprini: Writing – review & editing, Writing – original draft, Visualization, Software, Methodology, Investigation, Data curation, Conceptualization. **Morena Angelucci:** Writing – original draft, Visualization, Software, Methodology, Investigation, Data curation, Conceptualization. **Emanuela Martelli:** Writing – review & editing, Visualization, Software, Methodology, Investigation, Data curation, Conceptualization. **Fabio Crescenzi:** Writing – review & editing, Software, Methodology, Investigation, Data curation. **Francesco Giorgetti:** Writing – review & editing, Resources, Methodology. **Nicola Massanova:** Writing – review & editing, Resources. **Pietro Vinoni:** Writing – review & editing, Resources. **Domenico Marzullo:** Writing – review & editing, Resources. **Selanna Roccella:** Writing – review & editing, Validation, Supervision, Methodology, Conceptualization.

Declaration of competing interest

The authors declare that they have no known competing financial interests or personal relationships that could have appeared to influence the work reported in this paper.

Data availability

Data will be made available on request.

References

[1] F. Romanelli, et al., Divertor Tokamak Test facility Project: status of design and implementation, Nucl. Fusion. (2024), https://doi.org/10.1088/1741-4326/ad5740.
[2] R. Martone, R. Albanese, F. Crisanti, P. Martin, A. Pizzuto, DTT divertor tokamak test facility–Interim design report, ENEA (2019). DTT_IDR_2019_WEB.pdf.
[3] P.A. Di Maio, G. Mazzone, A. Quartararo, E. Vallone, J.H. You, Thermal-hydraulic study of the DEMO divertor cassette body cooling circuit equipped with a liner and two reflector plates, Fusion Eng. Des. 167 (2021) 112227, https://doi.org/10.1016/j.fusengdes.2021.112227.
[4] A. Quartararo, S. Basile, F.M. Castrovinci, P.A. Di Maio, M. Giardina, G. Mazzone, J.H. You, Thermofluid-dynamic assessment of the EU-DEMO divertor single-circuit cooling option, Fusion Eng. Des. 188 (2023) 113408, https://doi.org/10.1016/j.fusengdes.2022.113408.
[5] J.H. You, G. Mazzone, E. Visca, H. Greuner, M. Fursdon, Y. Addab, K. Zhang, Divertor of the European DEMO: engineering and technologies for power exhaust, Fusion Eng. Des. 175 (2022) 113010, https://doi.org/10.1016/j.fusengdes.2022.113010.
[6] S. Roccella, F. Giorgetti, R. De Luca, G. De Sano, G. Dose, P. Innocente, R. Neu, Armor thickness assessment for the Divertor Tokamak Test facility (DTT) Divertor targets, IEEE Trans. Plasma Sci. (2024), https://doi.org/10.1109/TPS.2024.3404135.
[7] Y. Seki, K. Ezato, S. Suzuki, K. Yokoyama, H. Yamada, T. Hirayama, T. Hirai, Numerical and experimental study of coolant water flow in ITER divertor outer vertical target, Fusion Eng. Des. 136 (2018) 420–425, https://doi.org/10.1016/j.fusengdes.2018.02.073.
[8] S. Kwon, H.T. Kim, S.H. Hong, S.W. Kwag, Y.B. Chang, N.H. Song, J. Jeong, Cfd analyses for the upgrade divertor system of kstar, Fusion Sci. Technol. 77 (7–8) (2021) 699–709, https://doi.org/10.1080/15361055.2021.1918960.
[9] P. Tarfila, O.C. Garrido, B. Končar, E. Martelli, F. Giorgetti, S. Roccella, Structural integrity evaluation of the DTT plasma facing unit using detailed CFD and thermo-mechanical analyses, Nuclear Mater. Energy 40 (2024) 101715, https://doi.org/10.1016/j.nme.2024.101715.
[10] J. Schlosser, et al., High heat flux tests at divertor relevant conditions on water-cooled swirl tube targets, in: Proc. 18th SOFT, 1994, pp. 40–43. https://inis.iaea.org/records/3xc0z-j3m76.
[11] A.R. Raffray, J. Schlosser, M. Akiba, M. Araki, S. Chiocchio, D. Driemeyer, D. Youchison, Critical heat flux analysis and R&D for the design of the ITER divertor, Fusion Eng. Des. 45 (4) (1999) 377–407, https://doi.org/10.1016/S0920-3796(99)00053-8.
[12] I. Smid, J. Schlosser, J. Boscary, F. Escourbiac, G. Vieider, Comparison between various thermal hydraulic tube concepts for the ITER divertor. Fusion Technology 1996, Elsevier, 1997, pp. 263–266. https://www.sciencedirect.com/science/article/abs/pii/B9780444827623500367?via%3Dihub.
[13] E. Rabaglino, (Italy)18th UIT Nat. Heat Transfer Conf.2000, 18th UIT Nat, Heat Transfer Conf (2000).
[14] J.H. You, H. Greuner, B. Böswirth, K. Hunger, S. Roccella, H. Roche, High-heat-flux performance limit of tungsten monoblock targets: impact on the armor materials and implications for power exhaust capacity, Nuclear Mater. Energy 33 (2022) 101307, https://doi.org/10.1016/j.nme.2022.101307.
[15] F. Escourbiac, A. Durocher, A. Fedosov, T. Hirai, R.A. Pitts, P. Gavila, A. Komarov, Assessment of critical heat flux margins on tungsten monoblocks of the ITER divertor vertical targets, Fusion Eng. Des. 146 (2019) 2036–2039, https://doi.org/10.1016/j.fusengdes.2019.03.094.